Manuscript version: Author's Accepted Manuscript

The version presented in WRAP is the author's accepted manuscript and may differ from the published version or Version of Record.

Persistent WRAP URL:

http://wrap.warwick.ac.uk/109017

How to cite:

Please refer to published version for the most recent bibliographic citation information.
If a published version is known of, the repository item page linked to above, will contain details on accessing it.

Copyright and reuse:

The Warwick Research Archive Portal (WRAP) makes this work by researchers of the University of Warwick available open access under the following conditions.

Copyright © and all moral rights to the version of the paper presented here belong to the individual author(s) and/or other copyright owners. To the extent reasonable and practicable the material made available in WRAP has been checked for eligibility before being made available.

Copies of full items can be used for personal research or study, educational, or not-for-profit purposes without prior permission or charge. Provided that the authors, title and full bibliographic details are credited, a hyperlink and/or URL is given for the original metadata page and the content is not changed in any way.

Publisher's statement:

Please refer to the repository item page, publisher's statement section, for further information.

For more information, please contact the WRAP Team at: wrap@warwick.ac.uk.

UAV-Aided MIMO Communications for 5G Internet of Things

Wei Feng, *Member, IEEE*, Jingchao Wang, Yunfei Chen, *Senior Member, IEEE*, Xuanxuan Wang,
Ning Ge, *Member, IEEE*, Jianhua Lu, *Fellow, IEEE*

Abstract—The unmanned aerial vehicle (UAV) is a promising enabler of the Internet of Things (IoT) vision, due to its agile maneuverability. In this paper, we explore the potential gain of UAV-aided data collection in a generalized IoT scenario. Particularly, a composite channel model including both the large-scale and the small-scale channel fading is used to depict typical propagation environments. Besides, not only the peak transmit power constraint but also the budget power and the total energy constraints are considered to characterize practical IoT devices. A multi-antenna UAV is employed, which follows a circular trajectory and visits the IoT devices in a sequential manner. For each transmission, the UAV communicates with a cluster of single-antenna IoT devices to form a virtual MIMO link. On these basis, we formulate a whole-trajectory-oriented optimization problem, where the transmission duration time and the transmit power of all devices are jointly designed for the whole flight. Different from previous studies, only the slowly-varying large-scale channel state information (CSI) is assumed available, to coincide with the fact that practically it is quite difficult to predictively acquire the random small-scale channel fading prior to the UAV flight. We propose an iterative scheme by leveraging the maxmin optimization and convex optimization tools, to overcome the non-convexity of the problem. The presented scheme adapts well to the rigorous energy constraints as well as the large-scale CSI condition, thus, it can provide a significant performance gain over traditional schemes and converges quickly.

Index Terms—*Internet of Things (IoT), unmanned aerial vehicle (UAV), energy constraint, MIMO, large-scale channel state information (CSI).*

I. INTRODUCTION

Nowadays, the unmanned aerial vehicle (UAV) has been widely investigated in conjunction with wireless communication networks [1], [2], [3], [4], as it can provide an on-demand flexible platform for deploying aerial base stations, or mounting mobile access points (APs) [5]. Particularly, the UAV has been recognized as one of the main key enablers of the Internet of Things (IoT) vision, thanks to its agile usability [6].

Different from the other applications of the ongoing Fifth Generation (5G) system, IoT devices are usually energy-limited [7], and they may be randomly scattered over a wide area for environmental monitoring or other targets. These issues will inevitably aggravate the coverage problem for IoT communications. By leveraging the UAV's agile mobility and maneuverability [8], it is a promising way to sequentially visit the IoT devices and move sufficiently close to the devices to collect the sensing data from them. Thus, the UAV-aided IoT communications may solve the coverage problem and significantly reduce the overhead of IoT communication networks. In addition, UAVs are cost-effective, which makes them suitable for emergency on-demand missions in IoT applications [9].

A. Related Work

Basically, the UAV can be either static at a fix location or mobile along a predefined/dynamically adjusted trajectory, providing static and mobile aerial APs, respectively. In the literature, many studies focused on the placement optimization problem of UAVs, which is an important issue for IoT applications. Particularly in [10], the authors presented an efficient analytical approach to optimize the altitude of UAV, which may improve the wireless coverage of aerial APs. Extending to the three-dimensional scenario, the authors of [11] formulated a UAV placement problem to maximize the revenue of the whole network, and proposed a computationally efficient numerical solution. In [12], the optimum placement of a relaying UAV for maximum reliability was studied, where the total power loss, the overall outage and the overall bit error rate were derived, and the optimum altitude was investigated for both static and mobile UAVs. The authors of [13] considered the problem of minimizing the number of UAVs while guaranteeing the wireless coverage performance, so as to further reduce the system cost.

These results have shown insightful results with respect to UAV's placement. However, the transmission strategies they assumed are all simple, which can not be directly applied to some severe IoT scenarios. Generally for IoT applications, the transmission strategy should be rigorously designed, so as to efficiently exploit the potential ability of energy-limited and randomly-scattered IoT devices.

Some researchers have also identified the difference in terms of transmission strategy optimization between UAV communications and traditional terrestrial communications. In [14], the authors studied a mobile relaying technique with high-mobility UAV relays. The end-to-end throughput was maximized via optimizing both the relay's trajectory as well as the source/relay's power allocation. Furthermore, the authors of [15] investigated the energy-efficient UAV communications

via trajectory optimization, where the propulsion energy consumption of UAVs was particularly considered. Therein, a theoretical model on the UAV's propulsion energy consumption was derived, based on which the energy efficiency of UAV communications was defined and then optimized. In [16], the authors maximized the approximate ergodic sum rate via dynamically adjusting the UAV heading. In [17], the minimum throughput over all ground users in the downlink UAV communication was maximized to achieve fair performance among users. These studies have uncovered useful researching points for the optimization of UAV communication strategies.

B. Main Contribution

Despite of the aforementioned fruitful results, utilizing UAV in an IoT scenario still faces some open challenges with respect to energy constraints of IoT devices as well as the channel model and the priori knowledge of channel state.

For IoT devices, not only the peak transmit power constraint, as considered in the previous studies, but also the total energy constraint, should be taken into account when optimizing the communication strategy, because for most cases, it is difficult to recharge the battery equipped at IoT devices. Besides, in IoT applications, the sensing data volume may dynamically change. Accordingly, the communication strategy should adapt to the data sensing status. In practice, a budget power constraint (more sensing data more budget power) can be introduced to simply link the communication strategy optimization and data sensing condition, which however is still untouched in the literature.

In order to depict a typical propagation environment for IoT applications, a practical channel model should be considered. In general, both the large-scale and the small-scale channel fading should be taken into account [18], [19]. As a contrast, quite a number of previous studies have assumed the free-space path-loss model to simplify mathematical analysis. Under the composite channel model, the priori knowledge for optimizing communication strategy should be carefully considered. Different from the free-space model, it becomes not feasible to assume perfect channel state information (CSI) in this case, because practically it is quite difficult to predictively acquire the random small-scale channel fading prior to the UAV flight. Towards this end, we can optimize the communication strategy in a whole-trajectory-oriented manner on the basis of only the slowly-varying large-scale CSI. However, to the best of the authors' knowledge, it is still an open issue to consider the composite channel model for UAV communications and perform optimization using the large-scale CSI only.

In this paper, we optimize the data collection efficiency of a UAV-aided IoT communication system, subject to a series of practical energy constraints as well as practical channel model and the large-scale CSI condition. The main contribution of this paper is summarized as follows.

- We consider a multi-antenna UAV, which follows a circular trajectory and visits the IoT devices in a sequential manner. For each transmission, the UAV communicates with a cluster of IoT devices. Thus, a virtual MIMO transmission link is formed, to adapt to the low transmit power

of IoT devices and enable multiple access within a time-frequency resource block. Both analysis and simulation results show that this operation is promising to improve the efficiency of sensing data collection.

- We consider a practical channel model consisting of both the large-scale and the small-scale channel fading, to characterize various propagation environments of IoT applications. In this case, the full CSI assumption, as used in most previous studies, becomes not applicable, as the fast-varying small-scale channel fading is difficult to obtain perfectly prior to the UAV flight. To this end, we assume that only the large-scale CSI is known. This is viable because the large-scale channel fading highly depends on the relative position of UAV and IoT devices, which can be calculated according to the historical channel sounding data together with the positional information of both UAV and IoT devices.

- We consider the peak transmit power, the budget power and the total energy constraints for IoT devices. Further based on the large-scale CSI condition, a whole-trajectory-oriented optimization problem is formulated to maximize the data collection efficiency by optimizing the transmission duration time of all devices, as well as their transmit power. Notably, in this work all the communication parameters are designed in a predefined manner, i.e., prior to the UAV flight. By adopting the random matrix theory, the maxmin optimization theory, as well as the convex optimization tools, we propose an efficient algorithm to solve the problem. Based on that, we also discuss the impact of UAV's deploying parameters on system performance.

C. Organization and Notation

The rest of the paper is organized as follows. Section II introduces the system model. The data collection efficiency of UAV-aided MIMO communications is analyzed and optimized in Section III. Section IV shows the simulation results and discussions, and finally, concluding remarks are given in Section V.

Throughout this paper, lower case and upper case boldface symbols denote vectors and matrices, respectively. $\mathbf{I}_N$ represents an $N \times N$ identity matrix, and $\mathbb{C}^{M \times N}$ represents the collection of all $M \times N$ complex matrices, and $\mathcal{CN}(0, \sigma^2)$ denotes the complex Gaussian distribution with zero mean and σ^2 variance. $(\cdot)^H$ and $(\cdot)^T$ represent the transpose conjugate and the transpose, respectively. $\mathbf{E}_x(\cdot)$ is the expectation operator with respect to x. $\det(\cdot)$ represents the determinant operator.

II. SYSTEM MODEL

As shown in Fig. 1, we consider a UAV-aided IoT communication system consisting of K IoT devices and an on-demand dispatched UAV. Due to the limited size of sensing devices, at each only a single antenna is equipped. The UAV, acting as an on-demand aerial AP, is equipped with M antennas, so as to promote the efficiency of data collection. Without loss of generality, we consider a circular coverage area centered at
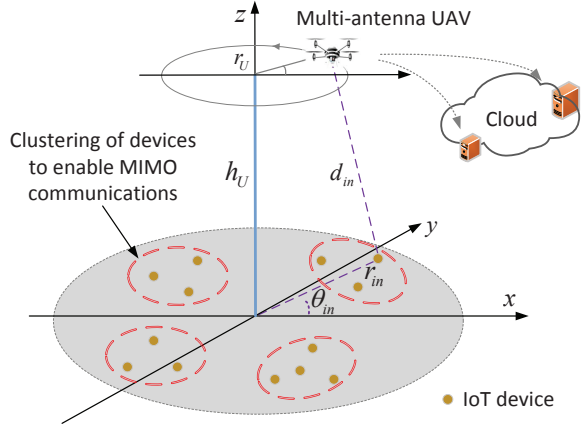
Fig. 1. Illustration of a UAV-aided IoT communication scenario, where the multi-antenna UAV servers as an on-demand aerial AP to communicate in a MIMO fashion with a cluster of IoT devices, and all the sensing data is collected, and forward to the cloud for further use.

(0, 0, 0), with a radius of r_c. All the devices are randomly deployed. The UAV flies right above the coverage area, at an altitude of h_U, following a circular trajectory of radius r_U centered at $(0, 0, h_U)$, with a duration time of T. In practice these parameters, i.e., h_U, r_U, T, are coupled with each other, influencing the total system performance, which should be carefully designed.

During the UAV flight, all the IoT devices will connect to the aerial AP when scheduled for data reporting[1]. We divide all the devices into orthogonal N clusters, each containing M adjacent devices, as shown in Fig. 1. In practice, these device clusters could be predefined for ease of management. At the cost of extra overhead, they can also be adjusted adaptively to fit with the UAV's dynamic position. For simplicity, we assume $K = MN$. Denote the polar coordinates of device i in cluster n as (r_{in}, θ_{in}). The corresponding rectangular coordinates would be $(r_{in}\cos(\theta_{in}), r_{in}\sin(\theta_{in}), 0)$. In this work, these N device clusters are scheduling in a round robin way under a time-division multiple access (TDMA) regime for fair access[2]. Particularly, if cluster n is scheduled, the corresponding M devices will simultaneously transmit data to the UAV, forming an $M \times M$ MIMO communication link. To be agile, the transmission duration time τ_n for cluster n is adjustable[3], while satisfying

$$\sum_{i=n}^{N} \tau_n \leq T. \tag{1}$$

As the total energy for data transmission for each device is quite limited, we assume both the peak transmit power

---

[1]The scheduling issue is also quite important, which however is out of the scope of this paper.

[2]In practice, when the number of IoT devices is much larger than UAV, non-orthogonal multiple access can be used [20], [21], which however would increase the processing complexity at the UAV.

[3]This is feasible in practice, where the velocity of the UAV can be dynamically controlled to fit this requirement.

constraint and the total energy constraint as

$$0 \leq p_{in} \leq P_{\max}, \quad \forall i, n, \tag{2}$$

$$p_{in}\tau_n \leq E_{\max}, \quad \forall i, n, \tag{3}$$

where p_{in} is the transmit power of device i in cluster n. Note that the transmission duration time is usually short in practice due to the energy constraint. Therefore, we assume that p_{in} maintains a constant during τ_i.

As discussed above, in IoT applications, the sensing data volume may dynamically change. Therefore, we introduce the budget power constraint P_{budget} to simply represent the current data sensing status. If there is only a little data to be reported, P_{budget} is set small for a longer life. Otherwise, P_{budget} should be set large enough for faster data reporting. We set

$$\sum_{i=1}^{M} p_{in} \leq P_{\text{budget}}, \forall n. \tag{4}$$

Different from previous studies, we consider a more practical channel model for all device-UAV links, by taking into account both the large-scale channel fading and the small-scale channel fading. As τ_i is short, we assume the opening angle of UAV with respect to the coordinate axis x is φ_n for cluster n when it is scheduled. Then the coordinates of UAV would be $(r_U\cos(\varphi_n), r_U\sin(\varphi_n), h_U)$. Accordingly, we have the distance between device i in cluster n and the mobile UAV as

$$d_{in} = \sqrt{h_U^2 + r_{in}^2 + r_U^2 - 2r_{in}r_U \cos\left(\varphi_n - \theta_{in}\right)}. \tag{5}$$

We consider both the line-of-sight (LOS) and non-line-of-sight (NLOS) channel elements, the large-scale path loss between device i in cluster n and the mobile UAV can be modeled as [10], [12]

$$L_{in}^{\text{dB}} = \frac{A}{1 + ae^{-b(\rho_{in}-a)}} + B_{in}, \tag{6}$$

where

$$A = \eta_{LOS} - \eta_{NLOS}, \tag{7}$$

$$B_{in} = 20\log_{10}(d_{in}) + 20\log_{10}(\frac{4\pi f}{c}) + \eta_{NLOS}, \tag{8}$$

$$\rho_{in} = \frac{180}{\pi} \arcsin(\frac{h_U}{d_{in}}), \tag{9}$$

and f is the carrier frequency, c is the speed of light. η_{LOS}, η_{NLOS}, a and b are constants related to the propagation environments [10], [12]. Consequently, the large-scale channel fading between device i in cluster n and the mobile UAV is derived as

$$L_{in} = 10^{-\frac{L_{in}^{\text{dB}}}{10}}. \tag{10}$$

Taking the Rayleigh small-scale channel fading into account, one may obtain the channel coefficient between device i in cluster n and the mobile UAV as

$$\mathbf{h}_{in} = L_{in}^{1/2}\mathbf{s}_{in}, \tag{11}$$

where $\mathbf{s}_{in} \in \mathbb{C}^{M\times 1}$, the entries of which are independent and identically distributed (i.i.d.) variables according to $\mathcal{CN}(0,1)$. Here, we use the Rayleigh fading to present the severe

propagation environment of IoT applications. For a more comprehensive study, the Rician fading [22], [23], as well as the Nakagami fading model [12] can be adopted.

Denoting the transmit signal of device i in cluster n by x_{in}, we have

$$\mathbf{E}\{|x_{in}|^2\} = p_{in}. \tag{12}$$

Based on the previous definitions, the received signal vector at the UAV from the device cluster n can be expressed as

$$\mathbf{y}_n = \mathbf{H}_n \mathbf{x}_n + \mathbf{n}_n, \tag{13}$$

where

$$\mathbf{H}_n = [\mathbf{h}_{1n}, \mathbf{h}_{2n}, ..., \mathbf{h}_{Mn}], \tag{14}$$
$$\mathbf{x}_n = [x_{1n}, x_{2n}, ..., x_{Mn}]^T, \tag{15}$$

and $\mathbf{n}_n$ represents the additive white Gaussian noise with independent entries distributed according to $\mathcal{CN}(0, \sigma^2)$.

For brevity, we set

$$\mathbf{H}_n = \mathbf{S}_n \mathbf{L}_n, \tag{16}$$

where $\mathbf{S}_n$ and $\mathbf{L}_n$ represent the small-scale and the large-scale channel coefficients, respectively, and

$$\mathbf{S}_n = [\mathbf{s}_{1n}, \mathbf{s}_{2n}, ..., \mathbf{s}_{Mn}], \tag{17}$$
$$\mathbf{L}_n = \begin{bmatrix} L_{1n}^{1/2} & & \\ & \ddots & \\ & & L_{Mn}^{1/2} \end{bmatrix}. \tag{18}$$

As $\mathbf{S}_n$ varies fast and is difficult to obtain in practice, we maximize the data collection efficiency of the considered system using only the slowly-varying large-scale CSI. In the following, both the transmission duration time and the transmit power of all devices for the whole flight will be optimized under realistic constraints of IoT applications.

III. OPTIMIZED UAV-AIDED MIMO COMMUNICATIONS

In this part, we first formulate a whole-trajectory-oriented optimization problem to maximize the data collection efficiency of UAV-aided MIMO communications. Then, we solve the non-convex problem in an iterative way, leading to an efficient resource allocation algorithm. The convergence of the algorithm is theoretically proved.

A. Problem Formulation

We maximize the data collection efficiency of the considered IoT model, subject to the UAV flying duration time constraint, the peak transmit power constraint and the total energy constraint of each device, as well as the budget power constraint of each device cluster. The problem is formulated as

$$\max_{\{\tau_n\}, \{p_{in}\}} \sum_{n=1}^{N} \tau_n R_n \tag{19a}$$

$$\text{s.t.} \sum_{n=1}^{N} \tau_n \le T, \tag{19b}$$

$$\tau_n \ge 0, \ \forall i, \tag{19c}$$

$$0 \le p_{in} \le P_{\max}, \ \forall i, \forall n, \tag{19d}$$

$$p_{in}\tau_n \le E_{\max}, \ \forall i, \forall n, \tag{19e}$$

$$\sum_{i=1}^{M} p_{in} \le P_{\text{budget}}, \forall n, \tag{19f}$$

where R_n denotes the achievable rate of device cluster n when it is scheduled. Since the small-scale CSI is unknown, R_n is calculated by taking expectation with respect to $\mathbf{S}_n$ as

$$R_n = \mathbf{E}_{\{\mathbf{S}_n\}}\left[\log_2 \det(\mathbf{I}_M + \frac{1}{\sigma^2}(\mathbf{S}_n\mathbf{L}_n)\mathbf{P}_n(\mathbf{S}_n\mathbf{L}_n)^H)\right], \tag{20}$$

where

$$\mathbf{P}_n = \begin{bmatrix} p_{1n} & & \\ & \ddots & \\ & & p_{Mn} \end{bmatrix}. \tag{21}$$

This problem is difficult to solve. On one hand, the objective function is implicit due to the expectation operator. On the other hand, the transmission duration time and transmit power are coupled with each other, rendering the problem non-convex, due to the constraints in (19e) [24].

B. Iterative Solution

The key difficulty of solving the problem in (19) lies in the coupling relationship between $\{\tau_n\}$ and $\{p_{in}\}$. Accordingly, we solve the problem in an iterative way, inspired by the idea of *divider and conquer*.

Let $s \ge 1$ denote the iterative step number. If $\{\tau_n^{s-1}\}$ is a feasible point of the problem, given $\{\tau_n^{s-1}\}$, we can simplify the problem as N subproblems as

$$\max_{\{p_{in}\}} R_n \tag{22a}$$

$$0 \le p_{in} \le P_{\max}, \ \forall i, \tag{22b}$$

$$p_{in}\tau_n^{s-1} \le E_{\max}, \ \forall i, \tag{22c}$$

$$\sum_{i=1}^{M} p_{in} \le P_{\text{budget}}, \forall n, \tag{22d}$$

$$n = 1, 2, ...N. \tag{22e}$$

Each subproblem is much simplified. However, it is still challenging due to the complicated objective function.

By adopting the random matrix theory [25], we derive an approximation for R_n as

$$R_n \approx \bar{R}_n = \sum_{i=1}^{M} \log_2(1 + \frac{1}{\sigma^2} L_{in} p_{in} \varpi^{-1} M)$$
$$+ M \log_2(\varpi_n) - M \log_2 e \left[1 - \varpi_n^{-1}\right], \tag{23}$$

where ϖ_n is the unique solution to the following fix-point equation [25]

$$\varpi_n = 1 + \sum_{i=1}^{M} \frac{L_{in}p_{in}}{\sigma^2 + L_{in}p_{in}\varpi_n^{-1}M}. \tag{24}$$

It has been identified that this approximation is quite accurate in the literature [26]. The performance gap is negligible in most cases. Thus by substituting $\bar{R}_n$ as the objective function, we can recast each subproblem as

$$\max_{\{p_{in}\}} \bar{R}_n \tag{25a}$$

$$0 \leq p_{in} \leq P_{\max}, \ \forall i, \tag{25b}$$

$$p_{in}\tau_n^{s-1} \leq E_{\max}, \ \forall i, \tag{25c}$$

$$\sum_{i=1}^{M} p_{in} \leq P_{\text{budget}}, \forall n, \tag{25d}$$

$$\varpi_n = 1 + \sum_{i=1}^{M} \frac{L_{in}p_{in}}{\sigma^2 + L_{in}p_{in}\varpi_n^{-1}M}, \tag{25e}$$

which however is still difficult to solve due to the constraint (25e). Basically, the constraint (25e) is a fixed-point equation, and we can leverage an iterative method to derive ϖ_n, as that in [26]. However, ϖ_n is coupled with the optimization variables $\{p_{in}\}$, making it an intractable obstacle for optimization.

To explore the relationship between $\bar{R}_n$ and ϖ_n, we obtain

$$\frac{d\bar{R}_n}{d\varpi_n} = -\frac{M\log_2 e}{\varpi_n^2} \sum_{i=1}^{M} \frac{L_{in}p_{in}}{\sigma^2 + L_{in}p_{in}\varpi_n^{-1}M}$$
$$+\frac{M\log_2 e}{\varpi_n} - \frac{M\log_2 e}{\varpi_n^2}. \tag{26}$$

Comparing (24) and (26), we get that $\frac{d\bar{R}_n}{d\varpi_n}$ is a monotonically increasing function of ϖ_n, and when the constraint (25e) holds,

$$\frac{d\bar{R}_n}{d\varpi_n} = 0. \tag{27}$$

These observations imply that $\bar{R}_n$ achieves its minimum with respect to ϖ_n for a given $\{p_{in}\}$. Thus, we further equivalently recast the problem in (25) as

$$\max_{\{p_{in}\}} \min_{\varpi_n} \bar{R}_n \tag{28a}$$

$$0 \leq p_{in} \leq P_{\max}, \ \forall i, \tag{28b}$$

$$p_{in}\tau_n^{s-1} \leq E_{\max}, \ \forall i, \tag{28c}$$

$$\sum_{i=1}^{M} p_{in} \leq P_{\text{budget}}, \forall n, \tag{28d}$$

$$\varpi_n \geq 1. \tag{28e}$$

Due to the convexity of log [24], [26], $\bar{R}_n$ is concave with respect to p_{in}. However, it is not a convex function of ϖ_n, which can be seen by deriving the second derivative of $\bar{R}_n$ with respect to ϖ_n (omitted here for brevity). This point makes it difficult to solve the problem in (28) using maxmin optimization tools [27].

We define a one-one mapping from ϖ_n to υ_n as

$$\varpi_n = e^{\upsilon_n}. \tag{29}$$

Then, from (23) (24), and (29), we have

$$\bar{R}_n = \sum_{i=1}^{M} \log_2(1 + \frac{1}{\sigma^2}L_{in}p_{in}e^{-\upsilon_n}M)$$
$$+M\log_2 e\upsilon_n - M\log_2 e\left[1 - e^{-\upsilon_n}\right], \tag{30}$$

$$\upsilon_n \geq 0. \tag{31}$$

Fortunately, we have

$$\frac{d\bar{R}_n}{d\upsilon_n} = -\frac{M\log_2 e}{e^{\upsilon_n}} \sum_{i=1}^{M} \frac{L_{in}p_{in}}{\sigma^2 + L_{in}p_{in}e^{-\upsilon_n}M}$$
$$+M\log_2 e - \frac{M\log_2 e}{e^{\upsilon_n}}, \tag{32}$$

and

$$\frac{d^2\bar{R}_n}{d\upsilon_n^2} = M\log_2 ee^{-\upsilon_n}$$
$$+M\log_2 e \sum_{i=1}^{M} \frac{L_{in}p_{in}\sigma^2 e^{\upsilon_n}}{\left(\sigma^2 e^{\upsilon_n} + L_{in}p_{in}M\right)^2}. \tag{33}$$

It is easy to see that

$$\frac{d^2\bar{R}_n}{d\upsilon_n^2} > 0. \tag{34}$$

Consequently, $\bar{R}_n$ is convex with respect to υ_n. On this basis, we recast the problem in (28) as

$$\max_{\{p_{in}\}} \min_{\upsilon_n} \bar{R}_n \tag{35a}$$

$$0 \leq p_{in} \leq P_{\max}, \ \forall i, \tag{35b}$$

$$p_{in}\tau_n^{s-1} \leq E_{\max}, \ \forall i, \tag{35c}$$

$$\sum_{i=1}^{M} p_{in} \leq P_{\text{budget}}, \forall n, \tag{35d}$$

$$\upsilon_n \geq 0, \tag{35e}$$

which becomes a typical maxmin optimization problem [27]. Because the objective function is concave with respect to the variable for maximization, and is convex with respect to the variable for minimization, the problem in (35) can be efficiently solved by classical maxmin optimization tools.

Then, we consider the optimization of $\{\tau_n\}$. If $\{p_{in}^{s-1}\}$ is a feasible point of the problem, given $\{p_{in}^{s-1}\}$, we can simplify the original problem in (19) as

$$\max_{\{\tau_n\}} \sum_{n=1}^{N} \tau_n \bar{R}_n \tag{36a}$$

$$\text{s.t.} \sum_{n=1}^{N} \tau_n \leq T, \tag{36b}$$

$$\tau_n \geq 0, \ \forall i, \tag{36c}$$

$$p_{in}^{s-1}\tau_n \leq E_{\max}, \ \forall i, \forall n, \tag{36d}$$

which fortunately is a convex optimization problem, thanks to the convexity of both objective function and constraints [24].

To solve the problem in (36) more efficiently, we re-order all the device clusters by

$$\bar{R}_1 \geq \bar{R}_2 \geq ... \geq \bar{R}_N. \tag{37}$$

Then, if

$$T \leq \min\left\{\frac{E_{\max}}{p_{11}^{s-1}}, \frac{E_{\max}}{p_{21}^{s-1}}, ..., \frac{E_{\max}}{p_{M1}^{s-1}}\right\}, \quad (38)$$

the optimal solution to (36) should be

$$\tau_1 = T,$$
$$\tau_n = 0, \ n > 1. \quad (39)$$

Otherwise, if

$$T \leq \min\left\{\frac{E_{\max}}{p_{11}^{s-1}}, \frac{E_{\max}}{p_{21}^{s-1}}, ..., \frac{E_{\max}}{p_{M1}^{s-1}}\right\}$$
$$+ \min\left\{\frac{E_{\max}}{p_{12}^{s-1}}, \frac{E_{\max}}{p_{22}^{s-1}}, ..., \frac{E_{\max}}{p_{M2}^{s-1}}\right\}, \quad (40)$$

the optimal solution to (36) should be

$$\tau_1 = \min\left\{\frac{E_{\max}}{p_{11}^{s-1}}, \frac{E_{\max}}{p_{21}^{s-1}}, ..., \frac{E_{\max}}{p_{M1}^{s-1}}\right\},$$
$$\tau_2 = T - \min\left\{\frac{E_{\max}}{p_{11}^{s-1}}, \frac{E_{\max}}{p_{21}^{s-1}}, ..., \frac{E_{\max}}{p_{M1}^{s-1}}\right\},$$
$$\tau_n = 0, \ n > 2. \quad (41)$$

In a similar fashion, if there exists $2 \leq \bar{N} \leq N$ that satisfies

$$T \leq \sum_{n=1}^{\bar{N}} \min\left\{\frac{E_{\max}}{p_{1n}^{s-1}}, \frac{E_{\max}}{p_{2n}^{s-1}}, ..., \frac{E_{\max}}{p_{Mn}^{s-1}}\right\},$$
$$T \geq \sum_{n=1}^{\bar{N}-1} \min\left\{\frac{E_{\max}}{p_{1n}^{s-1}}, \frac{E_{\max}}{p_{2n}^{s-1}}, ..., \frac{E_{\max}}{p_{Mn}^{s-1}}\right\}, \quad (42)$$

the optimal solution to (36) should be

$$\tau_n = \min\left\{\frac{E_{\max}}{p_{1n}^{s-1}}, \frac{E_{\max}}{p_{2n}^{s-1}}, ..., \frac{E_{\max}}{p_{Mn}^{s-1}}\right\}, n = 1 \sim \bar{N} - 1,$$
$$\tau_{\bar{N}} = T - \sum_{n=1}^{\bar{N}-1} \min\left\{\frac{E_{\max}}{p_{1n}^{s-1}}, \frac{E_{\max}}{p_{2n}^{s-1}}, ..., \frac{E_{\max}}{p_{Mn}^{s-1}}\right\},$$
$$\tau_n = 0, \ n > \bar{N} - 1. \quad (43)$$

Beyond that, i.e.,

$$T > \sum_{n=1}^{N} \min\left\{\frac{E_{\max}}{p_{1n}^{s-1}}, \frac{E_{\max}}{p_{2n}^{s-1}}, ..., \frac{E_{\max}}{p_{Mn}^{s-1}}\right\}, \quad (44)$$

the optimal solution to (36) should be

$$\tau_n = \min\left\{\frac{E_{\max}}{p_{1n}^{s-1}}, \frac{E_{\max}}{p_{2n}^{s-1}}, ..., \frac{E_{\max}}{p_{Mn}^{s-1}}\right\}, \forall n. \quad (45)$$

Based on the above analysis, we propose an iterative algorithm to solve the original problem in (19). In the presented algorithm, as shown in **Algorithm 1**, the transmission duration time $\{\tau_n\}$ and the transmit power $\{p_{in}\}$ are updated in an alternate fashion, until the achievable data collection efficiency of the system stops increasing. The achievable data collection efficiency of device cluster n calculated according to $\{p_{in}^s\}$ is denoted by $\bar{R}_n^s$.

It is clear that the achievable data collection efficiency is monotonically increasing in the iteration, i.e.,

$$\sum_{n=1}^{N} \tau_n^s \bar{R}_n^s \geq \sum_{n=1}^{N} \tau_n^{s-1} \bar{R}_n^{s-1}. \quad (46)$$

Algorithm 1 Solving (19) in an iterative way.

1: Initialization: $\tau_n^0 = \frac{T}{N}, \forall n$, $\epsilon = 1.0 \times 10^{-3}$, $s = 1$, $\bar{R}_n^0 = 0, \forall n$;
2: **for** $n = 1 \sim N$ **do**
3:     Solve the maxmin subproblem as shown in (35), and set the optimal result as $\{p_{in}^1\}$;
4: **end for**
5: **if** $T \leq \min\left\{\frac{E_{\max}}{p_{11}^1}, \frac{E_{\max}}{p_{21}^1}, ..., \frac{E_{\max}}{p_{M1}^1}\right\}$ **then**
6:     $\tau_1^s = T$, $\tau_n^s = 0$, $n > 1$;
7: **else**
8:     **if** $T > \sum_{n=1}^{N} \min\left\{\frac{E_{\max}}{p_{11}^1}, \frac{E_{\max}}{p_{2n}^1}, ..., \frac{E_{\max}}{p_{Mn}^1}\right\}$ **then**
9:         $\tau_n^s = \min\left\{\frac{E_{\max}}{p_{1n}^1}, \frac{E_{\max}}{p_{2n}^1}, ..., \frac{E_{\max}}{p_{Mn}^1}\right\}, \forall n$;
10:     **else**
11:         Find $\bar{N} \geq 2$ that satisfies
        $T \leq \sum_{n=1}^{\bar{N}} \min\left\{\frac{E_{\max}}{p_{1n}^1}, \frac{E_{\max}}{p_{2n}^1}, ..., \frac{E_{\max}}{p_{Mn}^1}\right\}$
        and $T \geq \sum_{n=1}^{\bar{N}-1} \min\left\{\frac{E_{\max}}{p_{1n}^1}, \frac{E_{\max}}{p_{2n}^1}, ..., \frac{E_{\max}}{p_{Mn}^1}\right\}$;
        Set $\tau_n^s = \min\left\{\frac{E_{\max}}{p_{1n}^1}, \frac{E_{\max}}{p_{2n}^1}, ..., \frac{E_{\max}}{p_{Mn}^1}\right\}$,
        $n = 1 \sim \bar{N} - 1$,
        $\tau_{\bar{N}}^s = T - \sum_{n=1}^{\bar{N}-1} \min\left\{\frac{E_{\max}}{p_{1n}^1}, \frac{E_{\max}}{p_{2n}^1}, ..., \frac{E_{\max}}{p_{Mn}^1}\right\}$,
        $\tau_n^s = 0$, $n > \bar{N} - 1$;
12:     **end if**
13: **end if**
14: **while** $|\sum_{n=1}^{N} \tau_n^s \bar{R}_n^s - \sum_{n=1}^{N} \tau_n^{s-1} \bar{R}_n^{s-1}| > \epsilon$ **do**
15:     $s = s + 1$;
16:     **for** $n = 1 \sim N$ **do**
17:         Solve the maxmin subproblem as shown in (35), and denote the optimal result as $\{p_{in}^s\}$;
18:     **end for**
19:     **if** $T \leq \min\left\{\frac{E_{\max}}{p_{11}^{s-1}}, \frac{E_{\max}}{p_{21}^{s-1}}, ..., \frac{E_{\max}}{p_{M1}^{s-1}}\right\}$ **then**
20:         $\tau_1^s = T$, $\tau_n^s = 0$, $n > 1$;
21:     **else**
22:         **if** $T > \sum_{n=1}^{N} \min\left\{\frac{E_{\max}}{p_{1n}^{s-1}}, \frac{E_{\max}}{p_{2n}^{s-1}}, ..., \frac{E_{\max}}{p_{Mn}^{s-1}}\right\}$ **then**
23:             $\tau_n^s = \min\left\{\frac{E_{\max}}{p_{1n}^{s-1}}, \frac{E_{\max}}{p_{2n}^{s-1}}, ..., \frac{E_{\max}}{p_{Mn}^{s-1}}\right\}, \forall n$;
24:         **else**
25:         Find $\bar{N} \geq 2$ that satisfies
        $T \leq \sum_{n=1}^{\bar{N}} \min\left\{\frac{E_{\max}}{p_{1n}^{s-1}}, \frac{E_{\max}}{p_{2n}^{s-1}}, ..., \frac{E_{\max}}{p_{Mn}^{s-1}}\right\}$
        and $T \geq \sum_{n=1}^{\bar{N}-1} \min\left\{\frac{E_{\max}}{p_{1n}^{s-1}}, \frac{E_{\max}}{p_{2n}^{s-1}}, ..., \frac{E_{\max}}{p_{Mn}^{s-1}}\right\}$;
        Set $\tau_n^s = \min\left\{\frac{E_{\max}}{p_{1n}^{s-1}}, \frac{E_{\max}}{p_{2n}^{s-1}}, ..., \frac{E_{\max}}{p_{Mn}^{s-1}}\right\}$,
        $n = 1 \sim \bar{N} - 1$,
        $\tau_{\bar{N}}^s = T - \sum_{n=1}^{\bar{N}-1} \min\left\{\frac{E_{\max}}{p_{1n}^{s-1}}, \frac{E_{\max}}{p_{2n}^{s-1}}, ..., \frac{E_{\max}}{p_{Mn}^{s-1}}\right\}$,
        $\tau_n^s = 0$, $n > \bar{N} - 1$;
26:         **end if**
27:     **end if**
28: **end while**
29: Output: $\{\tau_n^s\}$ and $\{p_{in}^s\}$.

Thus the proposed algorithm is guaranteed to converge, since the achievable data collection efficiency is upper bounded with given resources. In the following part, we will show that this algorithm may significantly increase the system performance, and it converges quickly.
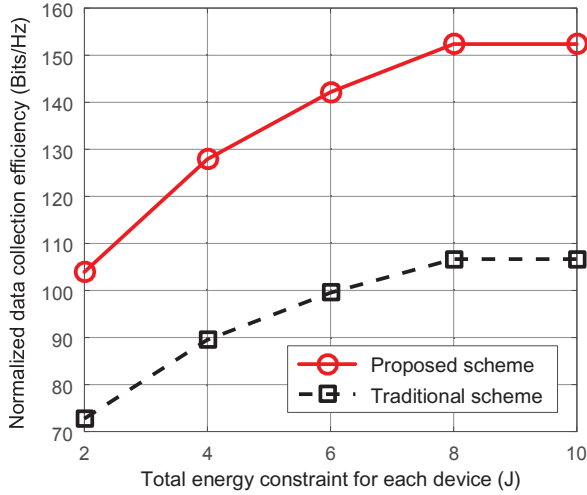
Fig. 2. Normalized data collection efficiency achieved by different schemes.

Fig. 3. Convergence performance of the propose scheme.

IV. SIMULATION RESULTS AND DISCUSSIONS

In this part, we evaluate the performance of the proposed algorithm by simulations and discus the influence of UAV deploying parameters on the system performance. We consider a circular coverage area. $K = 40$ single-antenna IoT devices are randomly deployed within the coverage area with Uninform Distribution. All the devices are divided into $N = 10$ independent clusters, each consisting of 4 devices. The UAV files right above the coverage area, at an altitude of $h_U = 800$ m, following a circular trajectory of radius $r_U = 1000$ m, with a duration time of $T = 1500$ s. The number of antennas at the UAV is $M = 4$. Thus, a 4×4 MIMO link is formed between an arbitrary device cluster and the UAV-mounted aerial AP.

As for the channel parameters, we set $f = 2$ GHz, $c = 3 \times 10^8$ m/s, $a = 5.0188$, $b = 0.3511$ [10]. Without loss of generality, we consider four typical urban environments using the following $(\eta_{LoS}, \eta_{NLoS})$ pairs $(0.1, 21)$, $(1.0, 20)$, $(1.6, 23)$, $(2.3, 34)$, corresponding to suburban, urban, dense urban, and highrise urban, respectively. For each IoT device, the peak transmit power is set as $P_{\max} = 300$ mw, i.e., 20 dBm. For each device cluster, we set $P_{\text{budget}} = 500$ mw. The noise power is set as $\sigma^2 = $ -107 dBm [26].

W first evaluate the performance of the proposed scheme with $(\eta_{LoS}, \eta_{NLoS}) = (0.1, 21)$. The averaged result of ten randomly-selected system topologies is shown in Fig. 2. In the traditional scheme, $\tau_n = \frac{T}{N}, \forall n$, and $p_{in} = \min\{P_{\max}, E_{\max}/\tau_n, P_{\text{budget}}/M\}$. This strategy is widely used in the literature when the large-scale CSI has not been taken into account. Note that the original problem shown in (19) is a non-convex optimization problem with an intractable objective function, therefore, it is too time-consuming to exhaustively search the optimal result. In the figure, the normalized data collection efficiency indicates $\sum_{n=1}^{N} \tau_n \bar{R}_n / K$. One can observe from the figure that the proposed scheme offers a significant performance gain over the traditional scheme. About 50% improvement is achieved when the total energy constraint equals to 4 J. Also, we can see that when the energy
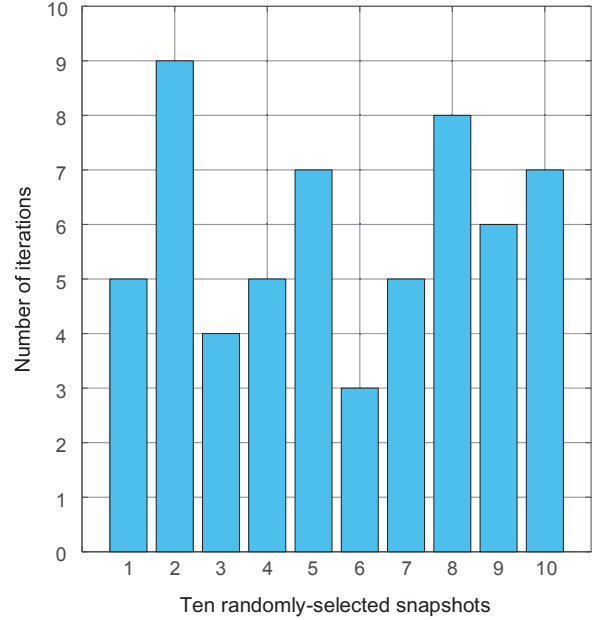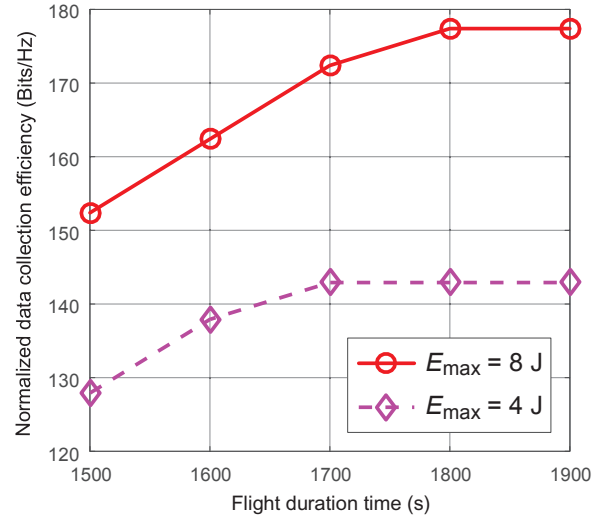

Fig. 4. Normalized data collection efficiency with different flight duration time.

constraint is larger than 8 J, the data collection efficiency will stop increasing. This is resulted by the peak transmit power constraint and the budget power constraint according to the volume of the sensing data.

In Fig. 3, we evaluate the convergence performance of the proposed scheme. When $E_{\max} = 4$ J, we show the number of iterations of ten randomly-selected system topologies. One may find from the figure that 10 iterations are enough to converge, and the average number of iterations is about 6. Recalling the previous mathematical work, we have decoupled the original problem into two parts, as shown in (35) and (36), respectively, both of which can be optimally solved. Moreover, the achievable data collection efficiency is monotonically
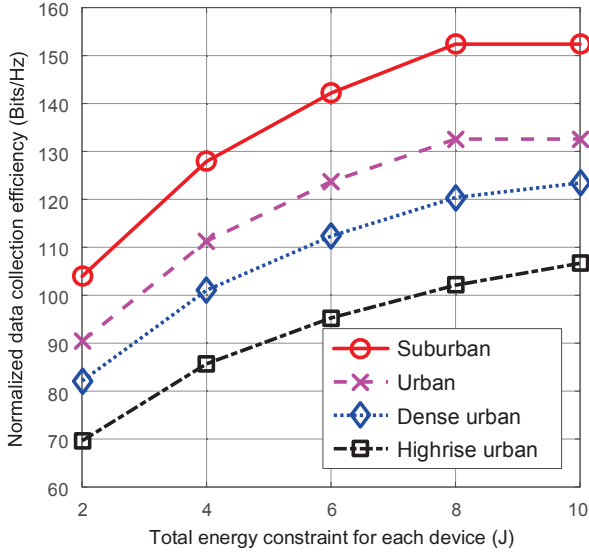
Fig. 5. Normalized data collection efficiency in different urban environments.
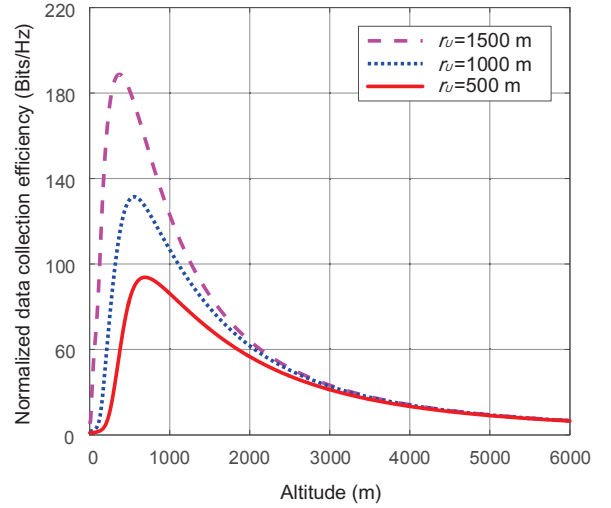

Fig. 6. Normalized data collection efficiency under different altitude of UAV.

Fig. 7. Normalized data collection efficiency under different radius of circular trajectory of UAV.

increasing in the iteration of the two subproblems. These facts largely lead to a good convergence performance. It implies that the proposed scheme can be used in practical applications where the computational resources is crucially limited for IoT, and the processing delay should be rigorously controlled.

As pointed out in section II that the flight duration time T is a quite important parameter influencing the system performance. In Fig. 4, we illustrate the normalized achievable data collection efficiency with different T. It is observed that given the total energy constraint, the achievable data collection efficiency will remarkably increase along with the increasing of T, especially when the total energy constraint is large. This is reasonable as a larger T means a larger optimization space for scheduling the transmit power, and the energy efficiency is accordingly improved. However, it makes no sense to continue to increase T when it is large enough, because the IoT system is essentially energy-limited. This is the reason for the performance ceiling in the figure, for both $E_{\max} = 4$ J and $E_{\max} = 8$ J.

In Fig. 5, we depict the achievable performance of the proposed scheme in different urban environments, i.e., with different $(\eta_{LoS}, \eta_{NLoS})$ values. It is seen from the figure that the performance gap is quite large between different environments. This fact indicates that it is quite necessary and meaningful to consider a practical channel model. This work investigates the composite channel model including both the large-scale and the small-scale channel fading, which is relevant to promote the application of UAV in IoT scenarios.

In Fig. 6 and Fig. 7, we further compare the achievable data collection efficiency of the proposed scheme under different altitude and under different radius of circular trajectory of the UAV, respectively. It can be seen from the figures that different deployment of UAV, i.e., different r_U and h_U, may lead to totally different system performance. In practice, these parameters should be carefully designed in a systematic way. Due to limited space, we do not further discuss these
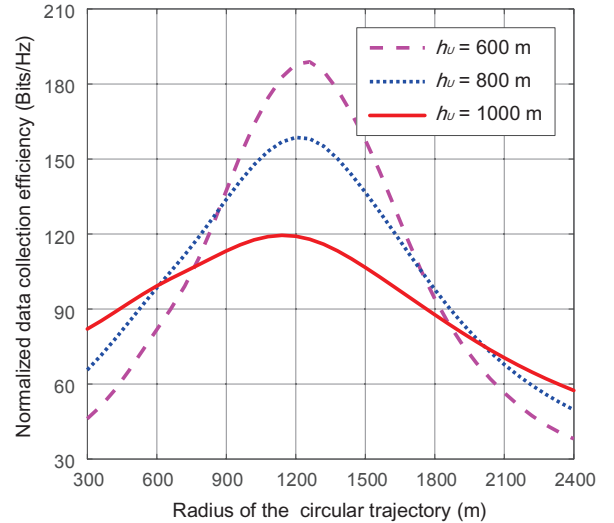
parameters theoretically. However, we believe that the optimal placement of the UAV under the considered framework is an interesting issue for future studies.

V. CONCLUDING REMARKS

In this paper, we focused on the application of UAV in IoT environments, where the UAV provides an agile on-demand platform for aerial APs to collect sensing data from the IoT devices. In particular, we have considered a composite channel model including both the large-scale and the small-scale channel fading, to depict practical propagation environments. We have also assumed the peak transmit power constraint, the budget power and the total energy constraints for realistic IoT devices. On these basis, a multi-antenna UAV was employed, which follows a circular trajectory and visits the IoT devices in a sequential manner. For each transmission,

the UAV communicates with a cluster of single-antenna IoT devices to form a virtual MIMO link. We have formulated a whole-trajectory-oriented optimization problem, where the transmission duration time and the transmit power of all devices are jointly designed for the whole flight. Different from previous studies, only the slowly-varying large-scale CSI was assumed available, to coincide with the practical difficulty in predictively acquiring the small-scale channel fading prior to the UAV flight. The problem is non-convex. To solve it, we have proposed an iterative scheme by leveraging the maxmin optimization and convex optimization tools. Simulation results have shown that the presented scheme adapts well to the rigorous energy constraints as well as the large-scale CSI condition, thus, it can provide a significant performance gain over traditional schemes and converges quickly.

Acknowledgment

References

[1] Q. Yu, J. Wang, and L. Bai, "Architecture and critical technologies of space information networks," *J. Commun. Info. Netw.*, vol. 1, no. 3, pp. 1–9, Sep. 2016.
[2] L. Bai, L. Zhu, X. Zhang, W. Zhang, and Q. Yu, "Multi-satellite relay transmission in 5G: concepts, techniques and challenges," *IEEE Netw. Mag.*, Sep. 2018.
[3] T. Qi, W. Feng, and Y. Wang, "Outage performance of non-orthogonal multiple access based unmanned aerial vehicles satellite networks," *China Commun.*, vol. 15, no. 5, pp. 1–8, May 2018.
[4] Q. Yu, C. Han, L. Bai, J. Choi, and X. Shen, "Low-complexity multiuser detection in millimeter-wave systems based on opportunistic hybrid beamforming," *IEEE Trans. Veh. Tech.*, 2018.
[5] Y. Zeng, R. Zhang, and T. J. Lim, "Wireless communications with unmanned aerial vehicles: opportunities and challenges," *IEEE Commun. Mag.*, vol. 54, no. 5, pp. 36–42, May 2016.
[6] N. Motlagh, T. Taleb, and O. Arouk, "Low-altitude unmanned aerial vehicles-based internet of things services: Comprehensive survey and future perspectives," *IEEE Intern. of Things J.*, vol. 3, no. 6, pp. 899–922, 2016.
[7] V. Sharma, R. Kumar, and R. Kaur, "UAV-assisted content-based sensor search in IoTs," *Electron. Lett.*, vol. 53, no. 11, pp. 724–726, 2017.
[8] S. Chandrasekharan, K. Gomez, A. Al-Hourani, S. Kandeepan, T. Rasheed, L. Goratti, L. Reynaud, D. Grace, I. Bucaille, T. Wirth, and S. Allsopp, "Designing and implementing future aerial communication networks," *IEEE Commun. Mag.*, vol. 54, no. 5, pp. 26–34, May 2016.
[9] N. Motlagh, M. Bagaa, and T. Taleb, "UAV-based IoT platform: A crowd surveillance use case," *IEEE Commun. Mag.*, vol. 55, no. 2, pp. 128–134, Feb. 2017.
[10] A. Al-Hourani, S. Kandeepan, and S. Lardner, "Optimal LAP altitude for maximum coverage," *IEEE Wireless Commun.*, vol. 3, no. 6, pp. 569–572, Dec. 2014.
[11] R. Bor-Yaliniz, A. El-Keyi, and H. Yanikomeroglu, "Efficient 3-D placement of an aerial base station in next generation cellular networks," in Proc. *IEEE Intern. Conf. Commun. (ICC)*, pp. 1–5, May 2016.
[12] Y. Chen, W. Feng, and G. Zheng, "Optimum placement of UAV as relays," *IEEE Commun. Lett.*, vol. 22, no. 2, pp. 248–251, 2018.
[13] J. Lyu, Y. Zeng, R. Zhang, and T. J. Lim, "Placement optimization of UAV-mounted mobile base stations," *IEEE Commun. Lett.*, vol. 21, no. 3, pp. 604–607, Mar. 2017.
[14] Y. Zeng, R. Zhang, and T. J. Lim, "Throughput maximization for UAV-enabled mobile relaying systems," *IEEE Trans. Commun.*, vol. 64, no. 12, pp. 4983–4996, Dec. 2016.
[15] Y. Zeng and R. Zhang, "Energy-efficient UAV communication with trajectory optimization," *IEEE Trans. Wireless Commun.*, vol. 16, no. 6, pp. 3747–3760, Jul. 2017.
[16] F. Jiang and A. L. Swindlehurst, "Optimization of UAV heading for the ground-to-air uplink," *IEEE J. Sel. Areas Commun.*, vol. 30, no. 5, pp. 993–1005, Jun. 2012.
[17] Q. Wu, Y. Zeng, and R. Zhang, "Joint trajectory and communication design for multi-UAV enabled wireless networks," *IEEE Trans. Wireless Commun.*, vol. 17, no. 3, pp. 2109–2121, 2018.
[18] Y. Zhang, W. Feng, and N. Ge, "Pilot power adaptation for tomographic channel estimation in distributed MIMO systems," *IET Commun.*, vol. 11, no. 1, pp. 112–118, Jan. 2017.
[19] C. Liu, W. Feng, T. Wei, and N. Ge, "Fairness-oriented hybrid precoding for massive MIMO maritime downlink systems with large-scale CSIT," *China Commun.*, vol. 15, no. 1, pp. 52–61, Jan. 2018.
[20] T. Qi, W. Feng, and Y. Wang, "Optimal sequences for non-orthogonal multiple access: a sparsity maximization perspective," *IEEE Commun. Lett.*, vol. 21, no. 3, pp. 636–639, Mar. 2017.
[21] T. Qi, W. Feng, Y. Chen, and Y. Wang, "When NOMA meets sparse signal processing: asymptotic performance analysis and optimal sequence design," *IEEE Access*, vol. 5, no. 1, pp. 18516–18525, 2017.
[22] J. Zhang, L. Dai, Z. He, S. Jin, and X. Li, "Performance analysis of mixed-ADC massive MIMO systems over Rician fading channels," *IEEE J. Sel. Areas Commun.*, vol. 35, no. 6, pp. 1327–1338, Jun. 2017.
[23] J. Zhang, X. Xue, E. Bjornson, B. Ai, and S Jin, "Spectral efficiency of multipair massive MIMO two-way relaying with hardware impairments," *IEEE Wireless Commun. Lett.*, vol. 7, no. 1, pp. 14–17, Feb. 2018.
[24] S. Boyd and L. Vandenberghe, *Convex optimization*, Cambridge University Press, 2004.
[25] A. M. Tulino and S. Verd, "Random matrix theory and wireless communications," *Found. Trends Commun. Inf. Theory,* vol. 1, no. 1, 2004.
[26] W. Feng, Y. Wang, N. Ge, J. Lu, and J. Zhang, "Virtual MIMO in multi-cell distributed antenna systems: coordinated transmissions with large-scale CSIT," *IEEE J. Sel. Areas Commun.*, vol. 31, no. 10, pp. 2067–2081, Oct. 2013.
[27] W. Sun, "On the convergence of an iterative method for the minimax problem," *J. Austral. Math. Soc. Ser. B*, vol. 39, no. 2, pp. 280–292, 1997.

Wei Feng (S'06-M'10) received his B.S. and Ph.D. degrees (both with the highest honor) from the Department of Electronic Engineering, Tsinghua University, Beijing, China, in 2005 and 2010, respectively. From 2010 to 2011, he served as a Project Director in the National Science and Technology Major Project Management Office of Tsinghua University. From 2011 to 2014, he was a Postdoctoral Research Fellow with the Department of Electronic Engineering, Tsinghua University, where he has been an Assistant Professor since Oct. 2014 and then an Associate Professor since Dec. 2016. His research interests include maritime broadband communication networks, large-scale distributed antenna systems, and coordinated satellite-terrestrial networks. He has published over 80 journal and conference papers. He also holds over 10 granted patents. Dr. Feng has received the Outstanding Ph.D. Graduate of Tsinghua University Award in 2010, the IEEE WCSP Best Paper Award in 2013, the first Prize of Science and Technology Award of China Institute of Communications in 2015, the IEEE WCSP Best Paper Award in 2015, and the second Prize of National Technological Invention Award of China in 2016. He currently serves as the Assistant to the Editor-in-Chief of China Communications.

Jingchao Wang received the Ph.D. degree in electronics engineering from Tsinghua University, Beijing, China. His research interests include space information networks and satellite communications.
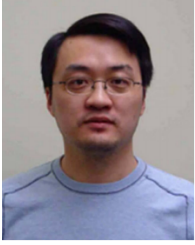
Yunfei Chen (S'02-M'06-SM'10) received his B.E. and M.E. degrees in Electronic Engineering from Shanghai Jiao Tong University, China, in 1998 and 2001, respectively. He received his Ph.D. degree from the University of Alberta, Canada, in 2006. He is currently working at the College of Computer and Information, Hohai University, Nanjing, China. He is also with the School of Engineering, Warwick University, Coventry, UK. His research interests include energy harvesting, wireless relaying and general performance analysis and design of wireless systems.

Xuanxuan Wang received the B.S. degree in communication engineering from Henan Polytechnic University, in 2010, and the M.S. degree in electronic and communication engineering from Beijing University of Posts and Telecommunications, Beijing, China, in 2013. She received the Ph.D. degree from Institute of Information and Engineering, Chinese Academy of Sciences, China, in 2017. She is currently a Postdoctoral Research Fellow with the Department of Electronic Engineering, Tsinghua University. Her current research interests include communication security, wireless information and power transfer, and convex optimization techniques.

Ning Ge (M'97) received his B.S. degree in 1993, and his Ph.D. in 1997, both from Tsinghua University, China. From 1998 to 2000, he worked on the development of ATM switch fabric ASIC in ADC Telecommunications, Dallas. Since 2000 he has been in the Dept. of Electronics Engineering at Tsinghua University. Currently he is a professor and also serves as Director of Communication Institute. His current interests are in the areas of communication ASIC design, short range wireless communication, and wireless communications. Dr. Ge is a senior member of CIC and CIE, and a member of the IEEE. He has published more than 100 papers.

Jianhua Lu (M'98-SM'07-F'15) received the B.S.E.E. and M.S.E.E. degrees from Tsinghua University, Beijing, China, in 1986 and 1989, respectively, and his Ph.D. degree in Electrical & Electronic Engineering from the Hong Kong University of Science & Technology in 1998. Since 1989, he has been with the Dept. of Electronic Engineering, Tsinghua Univ. Beijing, China, where he now serves as a Professor. His current research interests include broadband wireless communications, multimedia signal processing, and satellite communications. He is a Fellow of the IEEE. He has been an active member of professional societies and has published more than 200 technical papers in international journals and conference proceedings. He is a recipient of the best paper awards at the IEEE International Conference on Communications, Circuits and Systems 2002, ChinaCom 2006, and IEEE Embedded-Com 2012. He served in numerous IEEE conferences as a member of Technical Program Committees. He was an Editor of IEEE Transactions on Wireless Communications from 2008 to 2011, the Lead Chair of the General Symposium of IEEE ICC 2008, as well as a Program Committee Co-Chair of the 9th IEEE International Conference on Cognitive Informatics in 2010, and a general Co-Chair of the 14th IEEE International Conference on Cognitive Informatics in 2015. He is a member of Chinese Academy of Sciences. He has made influential contributions to China's national major engineering programs, such as the Lunar Program. He was awarded the second prize of National Technical Innovation Award, the second prize of National Natural Science Award of China. He was granted the funding of National Distinguished Young Scholar, and heading an Innovative Research Group of the National Natural Science Foundation of China. He was honored as the Yangtze River Scholar Distinguished Professor. He is now a chief scientist of the National Basic Research Program (973) of China, and also serves as an executive member of the council of Chinese Institute of Electronics-CIE, and a convener of discipline appraisal group of Information and Communication Engineering, Academic Degrees Committee of the State Council.